# Analysis of arterial sub-trees affected by Pulmonary Emboli

Atilla P. Kiraly[*a], Eric Pichon[b], David P. Naidich[c], Carol L. Novak[a]

[a]Siemens Corporate Research, 755 College Road East, Princeton, NJ 08540
[b]School of Electrical & Computer Engineering, Georgia Institute of Technology, Atlanta GA 30332
[c]Radiology Dept., New York University Medical Center, 560 First Avenue, New York, NY 10016

## ABSTRACT

Although Pulmonary Embolism (PE) is one of the most common causes of unexpected death in the U.S., it may also be one of the most preventable. Images acquired from 16-slice Computed Tomography (CT) machines of contrast-injected patients provide sufficient resolution for the localization and analysis of emboli located in segmental and sub-segmental arteries. After a PE is found, it is difficult to assess the local characteristics of the affected arterial tree without automation. We propose a method to compute characteristics of the local arterial tree given the location of a PE. The computed information localizes the portion of the arterial tree that is affected by the embolism. Our method is based on the segmentation of the arteries and veins followed by a localized tree computation at the given site. The method determines bifurcation points and the remaining arterial tree. A preliminary segmentation method is also demonstrated to locally eliminate over-segmentation of the arterial tree. The final result can then be used assess the affected lung volume and arterial supply. Initial tests revealed a good ability to compute local tree characteristics of selected sites.

**Keywords**: pulmonary embolism (PE), computed tomography (CT), tree analysis, center-line computation.

## 1. INTRODUCTION

Although Pulmonary Embolism (PE) is one of the most common causes of unexpected death in the U.S., it may also be one of the most preventable. Prompt treatment with anti-coagulants is essential to prevent loss of life; however treatments also carry risks, so correct diagnosis is critical. Computed tomography angiography (CTA) is gaining increasing acceptance as a method of diagnosis, offering sensitivity and specificity comparable or superior to alternative methods such as pulmonary angiography and ventilation-perfusion scans.[1,2] CTA is rapid and non-invasive, and in many cases has the benefit of allowing an alternative diagnosis to explain patients' symptoms.[3]

Images acquired from 16-slice Computed Tomography (CT) machines of contrast-injected patients provide very high-resolution data, allowing for better detection of emboli located in sub-segmental arteries.[4] The high resolution also offers the potential for a precise analysis of the effects of PEs on the lungs, but such assessments may be infeasible without automation.

Current research in automated analysis of PE within contrast-enhanced CT images concerns either the direct detection of the clots themselves within the arteries,[5,6] or indirect inference of clot location by visualization of perfusion defects in affected lung area(s).[7] In the former case, a good segmentation of the arteries is generally required in order to detect the precise locations of PEs. Once the PE candidates have been automatically identified, they are presented to users for verification. However up until now, the data used to detect PE locations has not been further analyzed for additional information.

In a parallel line of research into automated analysis of CTA, the mean density of local areas of the lungs are computed and rendered to directly visualize perfusion defects.[7] Lung areas showing lower than average density are suggestive of an upstream clot, although alternate causes such as emphysema need to be considered. An advantage of this technique is that it gives a graphical representation of the extent and severity of the disease.

[*] Atilla.Kiraly@siemens.com

We propose a method that bridges these two types of automated PE analysis. We make use of arterial tree extraction and specific clot locations as in the first type of analysis, but the goal is to quantify and visualize the extent of disease as in the second type of analysis. Specifically, we compute the characteristics of the local arterial tree associated with a pulmonary embolus, identified by either a physician or by automatic detection. This information presents a more detailed and potentially more accurate means of visualizing the physiologic consequences of central pulmonary embolism by delineating the extent of pulmonary arterial involvement. It is anticipated that this information will prove of value in assessing the clinical severity of disease as well as further refining prognosis.

In Section 2 we describe the details of this method. Results and preliminary conclusions are found in Sections 3 and 4, respectively.

## 2. METHODS

Our method takes two inputs and is composed of two modules. The inputs are the image volume and a selected point where a PE has occurred. The point may be manually indicated by a physician, or may be the output of an automatic detection algorithm. The first module performs segmentation and characterization of the entire lung vasculature. The second module involves computing the local tree characteristics given the selected point. These operations are depicted in Figure 1 and the following subsections describe these operations in detail.

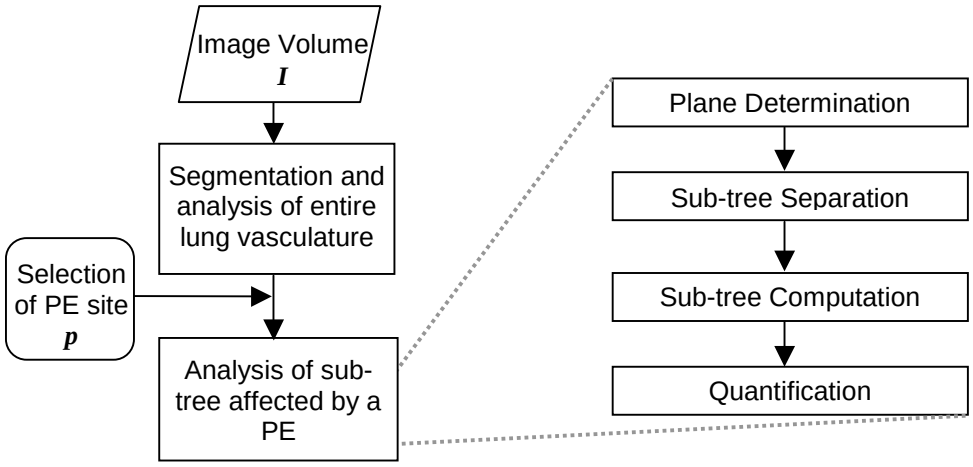


**Figure 1**: Operational diagram showing the two modules and two inputs. The four steps in the analysis of the sub-tree are presented on the right side.

The following notation will be used to describe the method. We refer to the original image volume by *I*. The selected PE site is given by $\boldsymbol{p}=(x,y,z)$. The volume containing the segmented vasculature within the lung is referred to as *S*. Finally, the segmented sub-tree volume is referred to as *S'*.

The first module for segmentation and characterization of the entire lung vasculature is described in detail in a related paper, but is briefly reviewed here.[8]

### 2.1. Segmentation and analysis of entire lung vessel tree

First, a mask of the lungs is created. A seed point is initially selected in the trachea. Region growing is then performed at this seed point until the entire lungs are segmented. This region growing involves a large threshold in order to fill the lungs via the airways. Dilation followed by erosion is then performed on the segmented image to fill empty spaces

caused by air-filled regions such as airways. The erosion operator is slightly larger than the dilation operator to prevent the ribs and other structures near the chest wall from being included in the mask.

Lung vessels are then segmented by including all voxels above a threshold value within the lung mask. The threshold is selected to include the denser vascular structures. Next a connected-component labeling is performed on the segmented structures. Structures with small volume are eliminated. The result is a segmentation of the pulmonary vasculature *S*. Currently a limitation is that pulmonary veins or other dense structures may be included along with arteries.

Next a Signed Distance Map $D_S$ is computed for the lung vessels. $D_S$ gives the distance of each voxel within *S* to the closest surface point. Larger arteries will have larger $D_S$ values at their core since they have larger radii. This information is used to compute the sub-tree.

At the end of this stage, we have the following data available for further processing:

1. Original contrast-enhanced CT image *I*
2. Segmentation of the lung vessels *S* containing distance labels $D_S$
3. A point ***p*** within the segmented image for further analysis

At this point, the analysis of the arterial tree affected by the PE can proceed.

### 2.2. Analysis of sub-tree affected by PE

The sub-tree analysis is composed of four steps, as shown on the right of Figure 1. First a bisecting plane perpendicular to the vessel's direction is determined at the point ***p***. This plane is used to perform a constrained region growing in Step 2 to isolate the distal portion of the tree, which we refer to as the *sub-tree*. A tree model is then calculated from the sub-tree via a skeletonization-based method, and analyzed to eliminate intersecting vessels. Finally, in Step 4, the affected lung volume is determined. The following describes each of these steps in detail.

#### 2.2.1. Plane Determination

The first step of the method is to determine the perpendicular plane of intersection with the selected point on the vessel. This plane is necessary for the next step. Given the selected point ***p***, a fixed-size sub-volume of the segmentation *S* is created about ***p***. Note that this fixed-size sub-volume only contains the local tree structure and not the complete tree in either proximal or distal directions. The segmented vasculature within this sub-volume is then modeled by a skeletonization-based tree computation method. We briefly describe this method with more detail found in a prior publication.[9]

The tree computation method computes a tree model given a segmented image of vasculature and a *root site*. A simple tree model is shown in Figure 2a. The tree is composed of a series of connected *branches*. Each branch, in turn, is composed of a series of *sites*. The root site defines the root of the tree and determines the parent-child relationships for all branches. The *branch site* is the site where branching occurs between two branches. Terminal sites are found at the end points of branches without children. Finally, all other sites are called viewing sites.

The following procedure determines the tree model. Given a segmented structure, its 3D skeleton is first computed. This operation converts the segmentation into a one-voxel thick structure composed of branching 3D lines. The skeleton is then stored into a tree model format where branches and branch points are found. The root site determines the root of the tree. The sites of each branch are the voxel locations forming a branch. This initial tree model most likely contains false branches due to the discrete nature of the data and the roughness of the segmentation. Using size-based criteria, false branches are deleted to refine the model. The site locations are also refined to a sub-voxel level. Finally, each site of the remaining branches also gets assigned a direction perpendicular to the branch direction on the basis of the locations of neighboring sites.

We apply this method to the sub-volume obtained about point ***p***. Our interest is in acquiring the perpendicular plane at location ***p***. The root site is simply chosen as the point within the segmentation furthest from ***p***. Note that this root site

may be incorrect with regard to the distal and proximal portions of the tree. The true root site should be located at the most proximal branch of the tree. However, the root site location does not influence the computed perpendicular plane at location ***p***. Given the computed model, we take the site closest to ***p*** and take the viewing direction of that site as the perpendicular to the plane. The next step uses this defined plane to cut the sub-tree from the rest of the tree.

Note that this tree computation method is also used in Step 3 to model the sub-tree. In the second usage of this method, the sub-tree segmentation obtained from Step 2 is used as input.

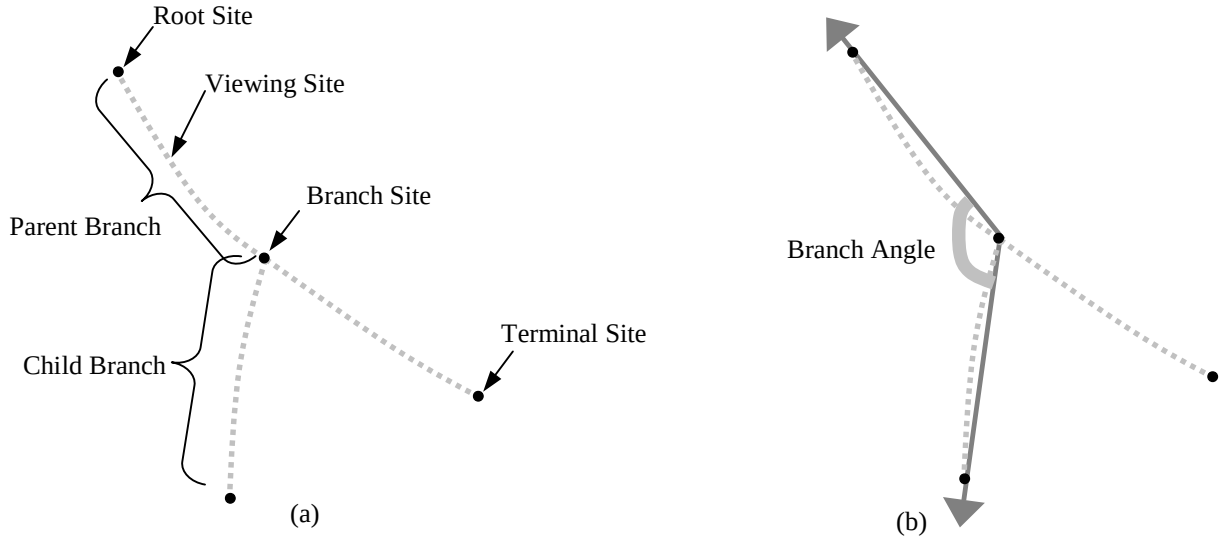


**Figure 2**: (a) Diagram of the anatomy of a simple tree model. A tree is composed of a series of connected branches. Various sites (viewing, root, terminal) form a branch. Each site contains directional information. The root site determines the base of the tree and defines the parent and child branch relationships for the remainder of the tree. (b) The branch angle definition: The branch angle is determined by the angle of the lines fitted to end sites of each branch. This branch angle definition works well for distal arteries since they are relatively straight.

### 2.2.2. Rule-based sub-tree separation

Given the plane that bisects the vessel, there is still the question of which side contains the sub-tree and which side contains the proximal vessels towards the heart. The purpose of this step is to produce the segmentation of the distal portion of the selected vasculature, which we refer to as *S'*.

Two rule-based region growing operations are performed on the segmented structure *S* at the location ***p***, one on each side of the plane. A standard 3D region growing operation is performed that is constrained in two ways. First, it must be bound by the segmentation defined in *S*. Second, the region may not cross the previously defined plane of Step 1. The smaller of the two regions is taken as the distal tree. The end result is a determination of the distal sub-tree $S' \subset S$, which is the basis for further processing. Note that this sub-tree may include additional vessels that appear to intersect due to partial volume effects. These issues are faced in the next step.

### 2.2.3. Sub-tree Computation

Given the sub-tree *S'*, its tree structure is determined by the tree computation method introduced in Step 1. Again, Step 1 only computed the tree structure about the selected point ***p***, not the entire sub-tree. The goal of this step is to provide a model of the sub-tree. The branch end point closest to the selected point ***p*** is automatically chosen as the root site for the model. However, the tree computation method assumes that the segmented tubular structure given as input forms a true tree and contains no overlapping structures. [9] This is not the case with all given sub-trees since the vessels of the

lungs may contain apparent overlaps due to partial volume effects. Hence, the computed model will contain incorrect branches into nearby vascular trees whenever such trees cross in *S'*.

Given the tree model of the segmentation, it is possible to determine vessel intersections due to nearby vessels. First, we determine the branch angles of each branch, as shown in Figure 2b. Figure 3 illustrates a method to identify and eliminate crossing vessels. The distal arterial tree has a branching structure that produces, in general, branch angles of greater than 90 degrees from the parent branch. Anytime a vessel from another sub-tree intersects within *S'*, it is captured in the tree structure. Any such intersections will produce branch angles less than 90 degrees along with a sibling branch with a supplementary branch angle. Hence, crossing vessels are identified as child branches having acute branch angles with siblings of supplementary branch angles. We allow a margin of error for the angles to be considered supplementary. Once crossing branches are identified, they are eliminated from the model. Note that the elimination of a branch from the tree model also requires the elimination of all of its child branches. Hence the deletion proceeds in an iterative fashion until the attached tree structure of the intersecting vessel is eliminated from the model as well.

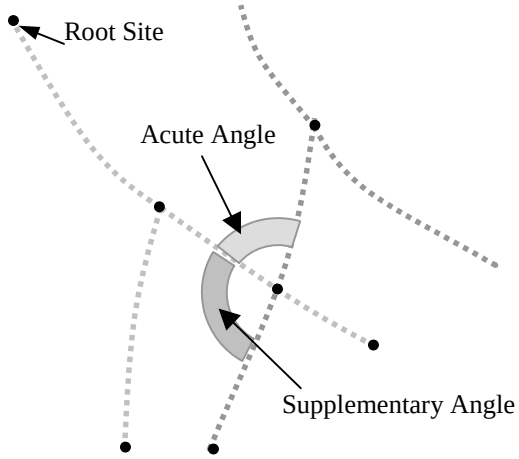


**Figure 3**: An example of the vessel intersection detection method used in Step 3. Due to partial volume effects, the segmentation may connect two vessels of different sub-trees. In this event, the model captures the nearby sub-tree as well. In this example, a vessel is intersecting at a site in a child branch. Figure 2a shows the true tree structure. The criterion for vessel intersection is an acute branch angle for a child branch along with a supplementary branch angle for one of its siblings. When this pattern is detected, the two branches are eliminated along with any attached branches. This method assumes that the vessels are relatively straight in the region of intersection.

The final tree model without any intersections can be used to refine the sub-tree defined in *S'*. Every site of every branch is associated with a distance value through $D_S$. Again, the distance values give the value of the shortest path from a given segmented voxel to the surface. Hence, the value is the radius of the largest sphere that can be contained within the segmentation at a particular voxel location. The availability of these distance values allows the tree model to recreate *S'* by placing appropriately sized spheres at each site in the model. Since intersecting trees are eliminated from the model, they will not appear in this recreated *S'*. The final *S'* then only contains the sub-tree without intersections. Hence, our initial determination of *S'* is not final and is further improved through high-level information available though the tree model.

### 2.2.4. Quantification

The quantification step estimates the region of the lung volume that is perfused by the sub-tree. In order to more accurately estimate this region, a detailed sub-tree involving the vessels near the chest wall is necessary. Although high resolution CT allows the extraction of small vessels, in most cases the segmented tree will not reach the chest wall. However, the segmentation comes sufficiently close to the wall to allow a good approximation of the affected volume.

Given each terminal branch (a branch with no children) in the tree model, we extend the branch in a linear fashion until it touches the chest wall. This method is illustrated in Figure 4. The terminal sites of each of these branches determine the direction of extension.

In order to determine the affected volume, we next compute the convex hull of this extended tree. This hull defines the affected region. The volume of this region is then measured and divided by the volume of the entire lung to give a percentage of the lung that is affected. We find the extension of the branches as an acceptable estimation since the branches are already near the chest wall. Any further branching most likely does not cross outside of the convex hull.

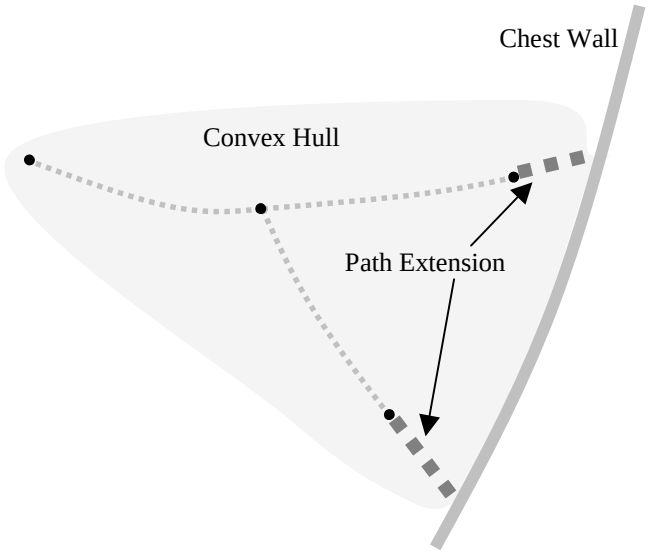


**Figure 4**: An example of the computation of the affected lung region. The terminal branches of the tree model are first linearly extended until they touch the chest wall. The direction of extension is determined by the end points of each branch. This extension is used to estimate the localization of the vessels near the chest wall. A 3D convex hull is then fit to the sub-tree and used to estimate the volume of lung perfused by that sub-tree.

### 2.2.5. Visualization

The images generated by the above method are displayed to the user to give graphical feedback of the results of the segmentation and quantification. We determined the following presentation based on physician recommendations. The segmented arteries are displayed in a transparent color. The convex hull of the sub-segmented tree is used to visualize the affected region. This region combined with the transparent view of the lung gives a visual display of the affected volume of the lung.

### 2.2.6. Iteration

For clarity, the previous discussion has focused upon a single PE site and the extracted sub-tree. However many patients have multiple PEs. The steps above can be repeated for additional selected PE sites, with a new sub-tree extracted for each site. The volumes subtended by each of the sub-trees may be summed together to indicate the total affected lung volume.

In the case where an indicated PE is directly downstream of another, one sub-tree will be completely contained within another. This condition is easy to detect from the tree computation. In this case, the volume of the smaller tree is not added to the larger to compute the total affected percentage.

Figure 5 demonstrates the steps of the method on real patient data.

## 3. RESULTS

This section presents some preliminary results of our method. Preliminary testing shows that local tree structure computation is feasible within a given segmentation. Our final sub-tree segmentation demonstrates a good potential for the arterial trees. Nearby intersecting vessels are successfully detected and eliminated. A step-by-step example of the method and the user interaction is shown in Figure 5. For this example, the algorithm computed that 5.7 percent of the lung was affected by the indicated PE.

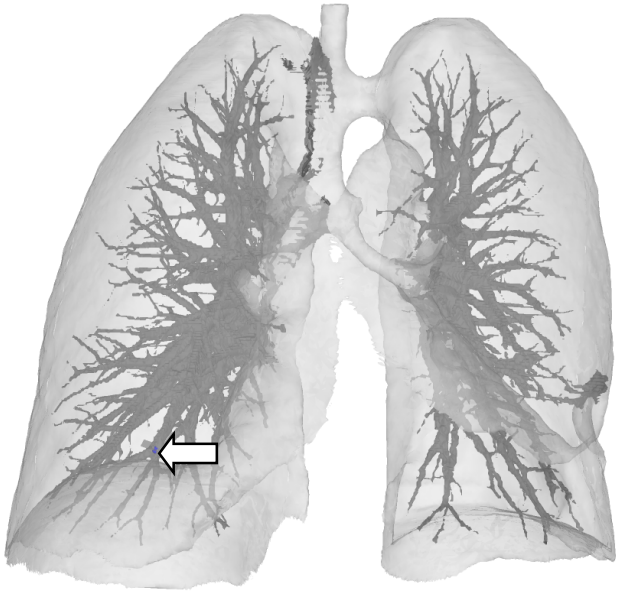

**Figure 5a**: The extracted arteries and the lung mask, along with a selected PE site indicated by an arrow.

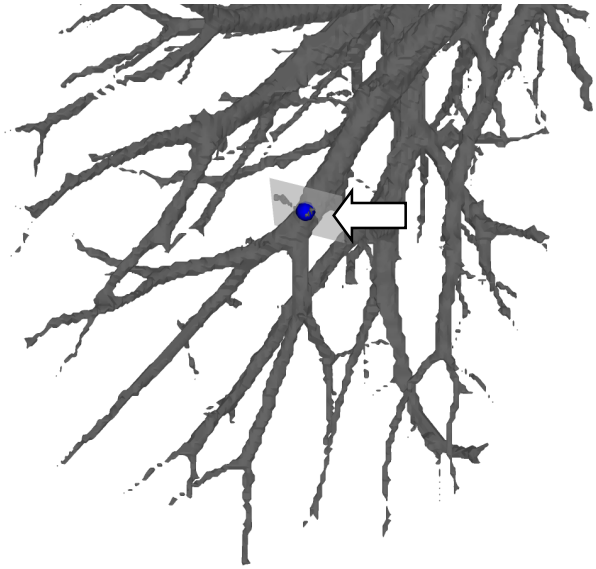

**Figure 5b**: The perpendicular plane to the selected site is computed.

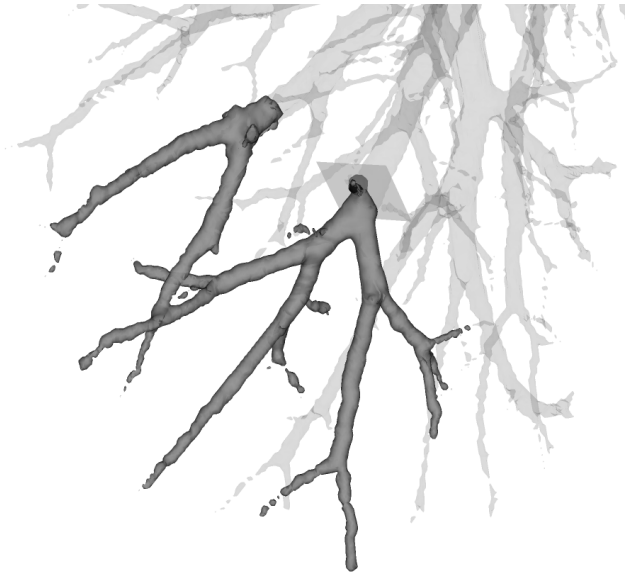

**Figure 5c**: The separated sub-tree, shown in context with the rest of the tree.

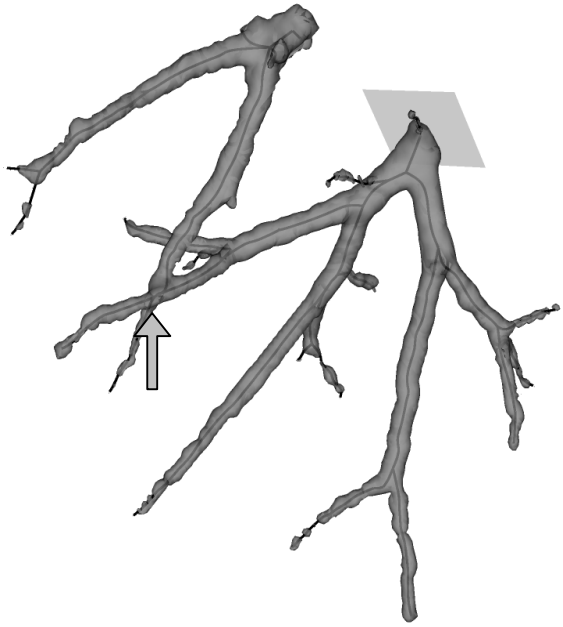

**Figure 5d**: The sub-tree alone, shown with its computed tree model. Notice the crossing branch of another sub-tree.

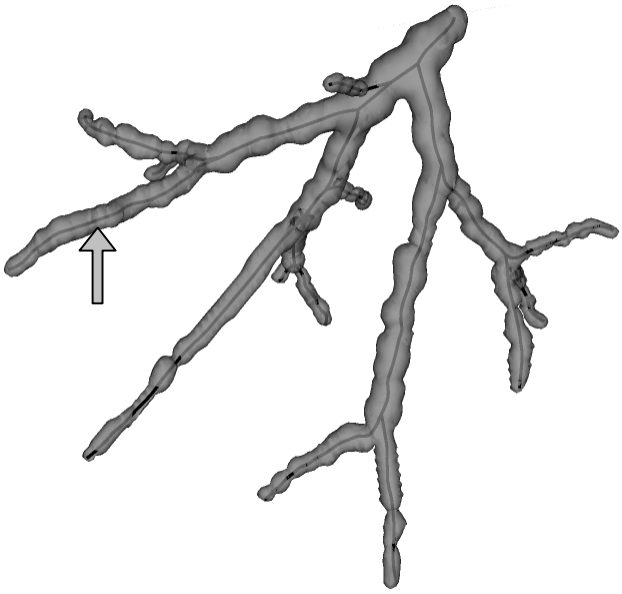

**Figure 5e**: The sub-tree after removal of the crossing branch.

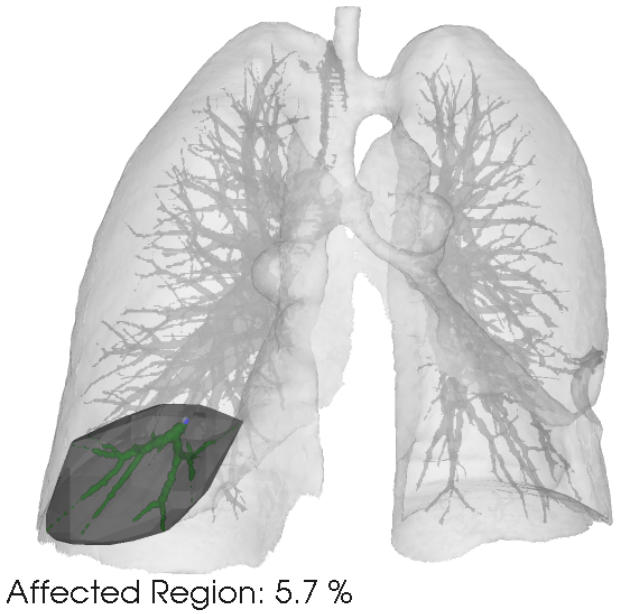


**Figure 5f**: The convex hull of the extended sub-tree is determined to visualize and compute the percentage of affected lung.

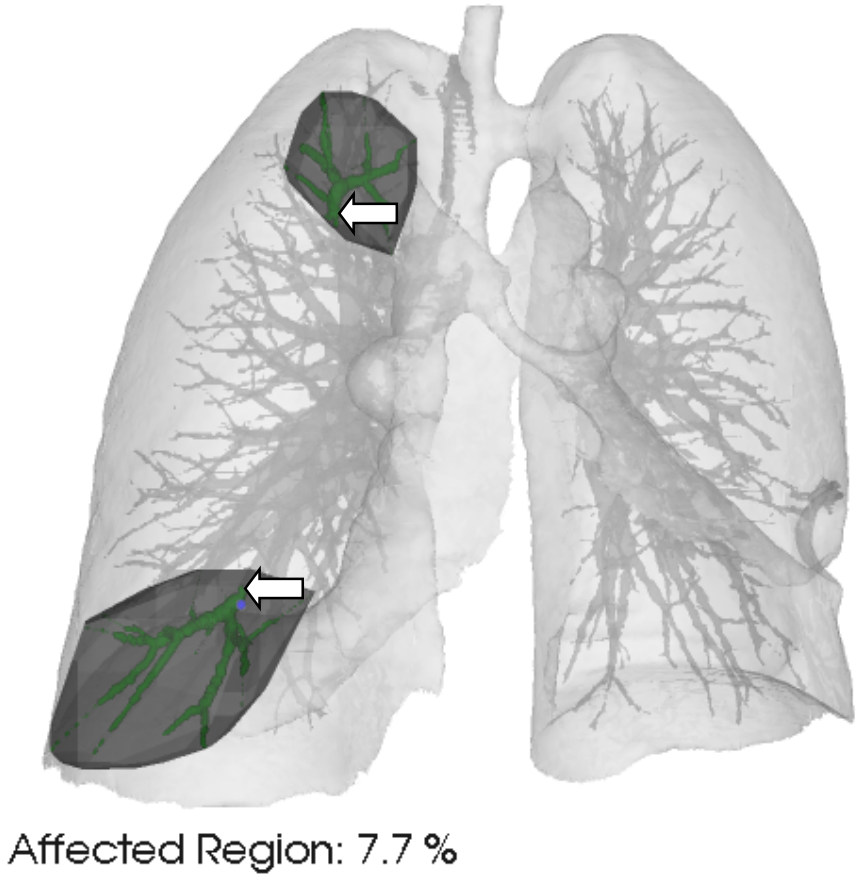


**Figure 6**: Visualization of lungs affected by two clots.

Figure 6 shows the same patient, but where the user has selected two PE sites. In this example, the computer calculated the affected lung as 7.7 percent of the total lung volume.

## 4. CONCLUSIONS AND FUTURE WORK

Although intraluminal clot within the proximal pulmonary arterial tree is generally readily identifiable on routine cross-sectional images, optimal assessment of the true extent of arterial involvement is best performed with 3-dimensional visualization. We describe a novel approach for localized arterial tree assessment given prior identification of pulmonary emboli, using plane determination, rule-based segmentation, and tree computation to identify the remaining arterial tree. The data gathered from the sub-tree is not only useful for physician evaluation, but can also be used as features for improved classification in PE detection systems.

While preliminary results of this method demonstrate its feasibility, the following improvements should further refine our method. These include improved segmentation of both the lungs and vasculature. The lung segmentation can be refined by delineating the locations of fissures. Knowing the lobar boundaries will allow additional constraints for computing the affected sub-volume. Improved vascular segmentation will also benefit the estimation of the affected volume.

Image resolution and partial volume effects limit the segmentation of peripheral arteries. Improved segmentation would involve combining our approach with alternative segmentation techniques that may enhance results in the sub-voxel range. The problem domain is further constrained since we are only interested in the sub-tree. Vessel tracking techniques may be used at the terminal branches in a way to combine its advantages with that of region growing through a high-level tree model. The starting point and direction of the sub-tree is available and can be used for improved results.

While it remains to be determined whether our method of 3 dimensional computation of the peripheral pulmonary arterial tree will prove of clinical value, it is anticipated that a more accurate estimate of the extent of arterial involvement following pulmonary embolism will lead to further refinements in both therapy and prognosis.

Even given the improved segmentations, determining the affected lung region presents a difficult task with the limited resolution of the data. The arterial branches may fall near each other, making it difficult to determine exactly which region is covered by which arterial tree. Characterizing the extracted vasculature as a “tree” may be something of a misnomer, since in many cases the segmentation will contain cycles due to the apparent crossings. We showed that in some cases these cycles may be detected by examining the branch angles to detect a phantom crossing. We anticipate that use of the distance labels within the segmentation can also be employed to detect branches that are headed proximally instead of peripherally. The use of branch angles and distance labels to help detect crossings may also be useful in artery-vein separation on the scale of the entire tree structure.

## REFERENCES


1. Mayo JR, Remy-Jardin M, Muller NL, Remy J, Worsley DF, Hossein-Foucher C, Kwong JS, Brown MJ, “Pulmonary Embolism: Prospective Comparison of Spiral CT with Ventilation-Perfusion Scintigraphy”, *Radiology*; **205**: 447-452, 1997.
2. Remy-Jardin M, Remy J, Deschildre F, Artaud D, Beregi JP, Hossein-Foucher C, Marchandise X, Duhamel A, “Diagnosis of Pulmonary Embolism with Spiral CT: Comparison with Pulmonary Angiography and Scintigraphy”, *Radiology* **200**:699-706, 1996.
3. Kim KI, Muller NL, Mayo JR, “Clinically suspected pulmonary embolism: utility of spiral CT”, *Radiology* 210(3): 693-7, 1999.
4. Schoepf UJ, Holzknecht N, Helmberger TK, Crispin A, Hong C, Becker CR, Reiser MF, “Subsegmental pulmonary emboli: improved detection with thin-collimation multi-detector row spiral CT”, *Radiology* 222(2): 483-90, 2002**.**

5. Masutani Y, MacMahon H, Doi K, "Computerized detection of pulmonary embolism in spiral CT angiography based on volumetric image analysis," *IEEE Trans. Med. Imaging*, **21(12)**: 1517-1523, 2002.
6. Zhou C, Hadjiiski LM, Sahiner B, Chan HP, Patel S, Cascade PN, Kazerooni EA, Wei J, "Computerized detection of pulmonary embolism in 3D Computed Tomographic (CT) images: vessel tracking and segmentation techniques," *SPIE Medical Imaging 2003*, **5032**: 1613-1620, 2003.
7. Wildberger JE, Niethammer MU, Klotz E, Schaller S, Wein BB, Gunther RW, "Multi-slice CT for visualization of pulmonary embolism using perfusion weighted color maps", *Rofo Fortschr Geb Rontgenstr Neuen Bildgeb Verfahr* **173(4)**: 289-94, 2001.
8. Pichon E, Novak CL, Kiraly AP, Naidich DP, "A novel method for pulmonary emboli visualization from high-resolution CT images," *SPIE Medical Imaging 2004*, **5367,** 2004.
9. Kiraly AP, Higgins WE, "Analysis of branching tubular structures in 3D digital images**"**, *Proceedings, International Conference on Image Processing 2002*, Piscataway, NJ: IEEE Press, **2**: 333-336, 2002.